# Supplementary Information

## Effect of the Development of a Cell Barrier on Nanoparticle Uptake in Endothelial Cells

*Valentina Francia, Aldy Aliyandi, and Anna Salvati*

| Gene | Forward (left) | Reverse (right) |
|---|---|---|
| CAV1 | ACAGCCCAGGGAAACCTC | GATGGGAACGGTGTAGAGATG |
| CDC42 | CATCGGAATATGTACCGACTGTT | TGCAGTATCAAAAAGTCCAAGAGTA |
| CLTC | TGAGAAAAGAAGAAGAACAAGCTACA | ACACTGGGTCCTGCTGTCA |
| RHOA | GGAGCTAGCCAAGATGAAGC | GCCAATCCTGTTTGCCATA |
| ARF6 | TGAACACAAAGTTGCTAGATGCT | TGCTGTGTTTCCCCCATC |
| TFRC | TGAAGAGAAAGTTGTCGGAGAAA | CAGCCTCACGAGGGACATA |
| DNM2 | CATCAACACGAACCATGAGG | CTTGTTCAGCTGCGTGCTC |
| FLOT1 | ATTCTAACTCGCCTGCCAGA | GCATCTGTGAGGGCTGAAG |
| LDLR | GTGACAATGTCTCACCAAGCTC | CACGCTACTGGGCTTCTTCT |
| GRAF1 | CAGGCACGGTCTTCGATAA | GCCAGTCTTTCCGTTCAGAG |
| RAC1 | CTGATCAGTTACACAACCAATGC | CATTGGCAGAATAATTGTCAAAGA |
| ANKFY1 | AAACTAGCAAATCGGTTTCAGC | GAGACATAACACCCTTCTCACATC |
| EPN1 | GAGAGCAAGAGGGAGACTGG | AAGACGTCAGCAAGGTCCAT |

**Table S1.** Primers used in this study for RT-qPCR. RT-qPCR was performed as described in the Experimental Section to determine the expression levels of genes coding for cell receptors (LDL and transferrin receptor) and for a series of targets involved in different endocytic pathways.

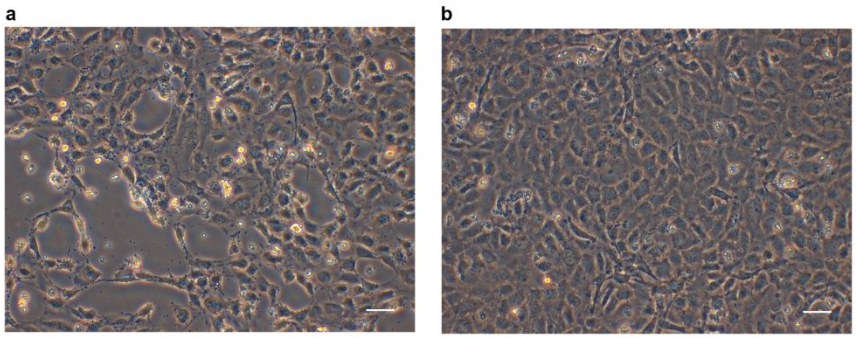


**Figure S1.** Effect of surface coating on cell growth. Representative light microscopy images of HUVEC plated at a concentration of 10000 cells $cm^{-2}$ on 24 well plates uncoated (a) or coated with rat tail collagen Type-I (b) (scale bar 50 μm). The presence of a collagen coating clearly improved cell adherence and cell growth.

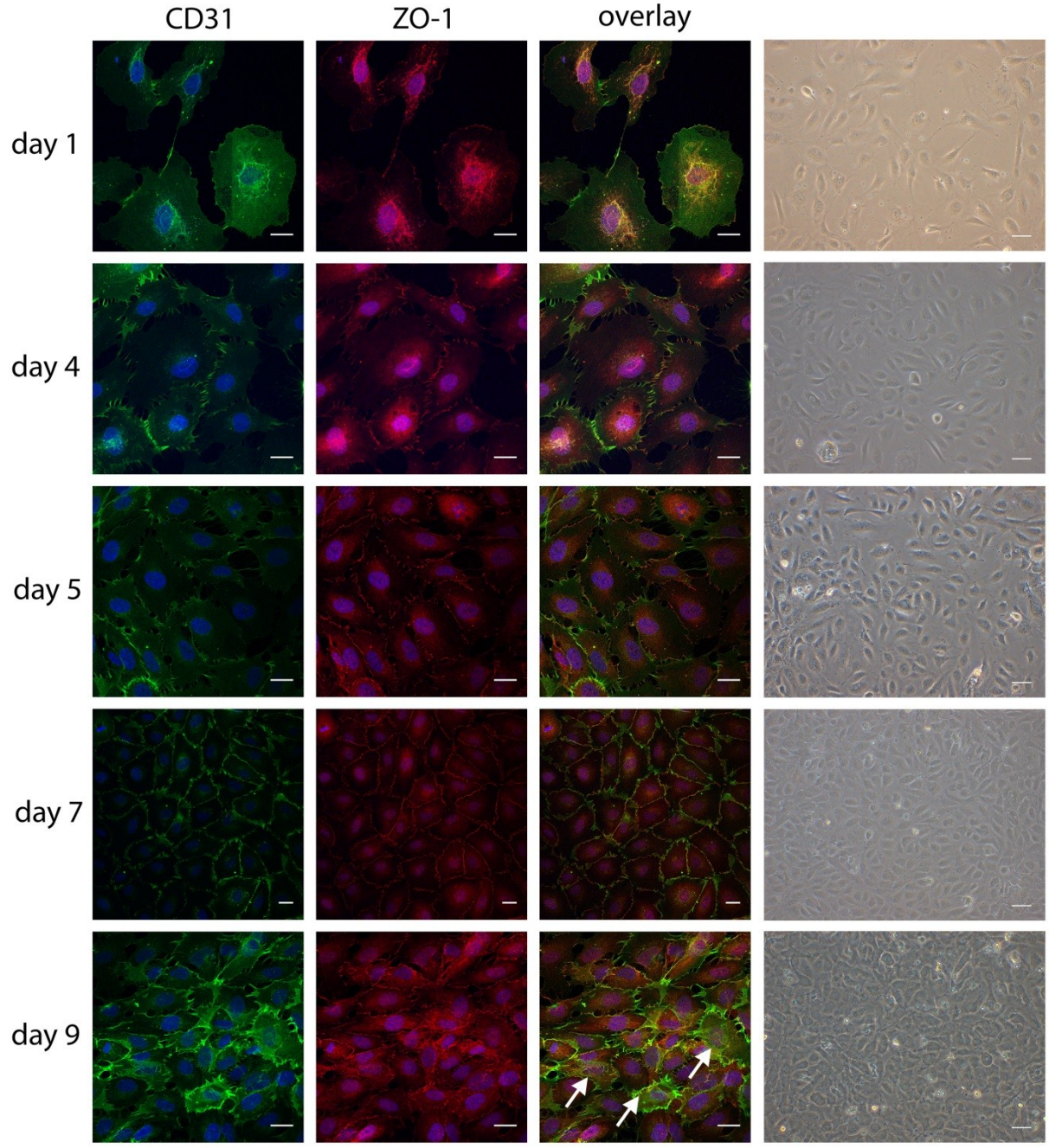


**Figure S2.** HUVEC barrier formation from low cell density cultures. 3000 cells $cm^{-2}$ HUVEC were plated on collagen coated glass coverslips and their growth was monitored for different days after seeding. Left: confocal images of HUVEC cells stained with anti-ZO-1 (red) or anti-CD31 (green) antibodies. Blue: DAPI stained nuclei (scale bar: 20 μm). Right: light microscopy images of the same cultures (scale bar: 50 μm). Tight junction staining showed barrier formation roughly 7 days after cell seeding, then cells started to overlap in multiple layers (as indicated by white arrows) and areas with holes in the cell monolayer were observed, as a consequence of cell death.

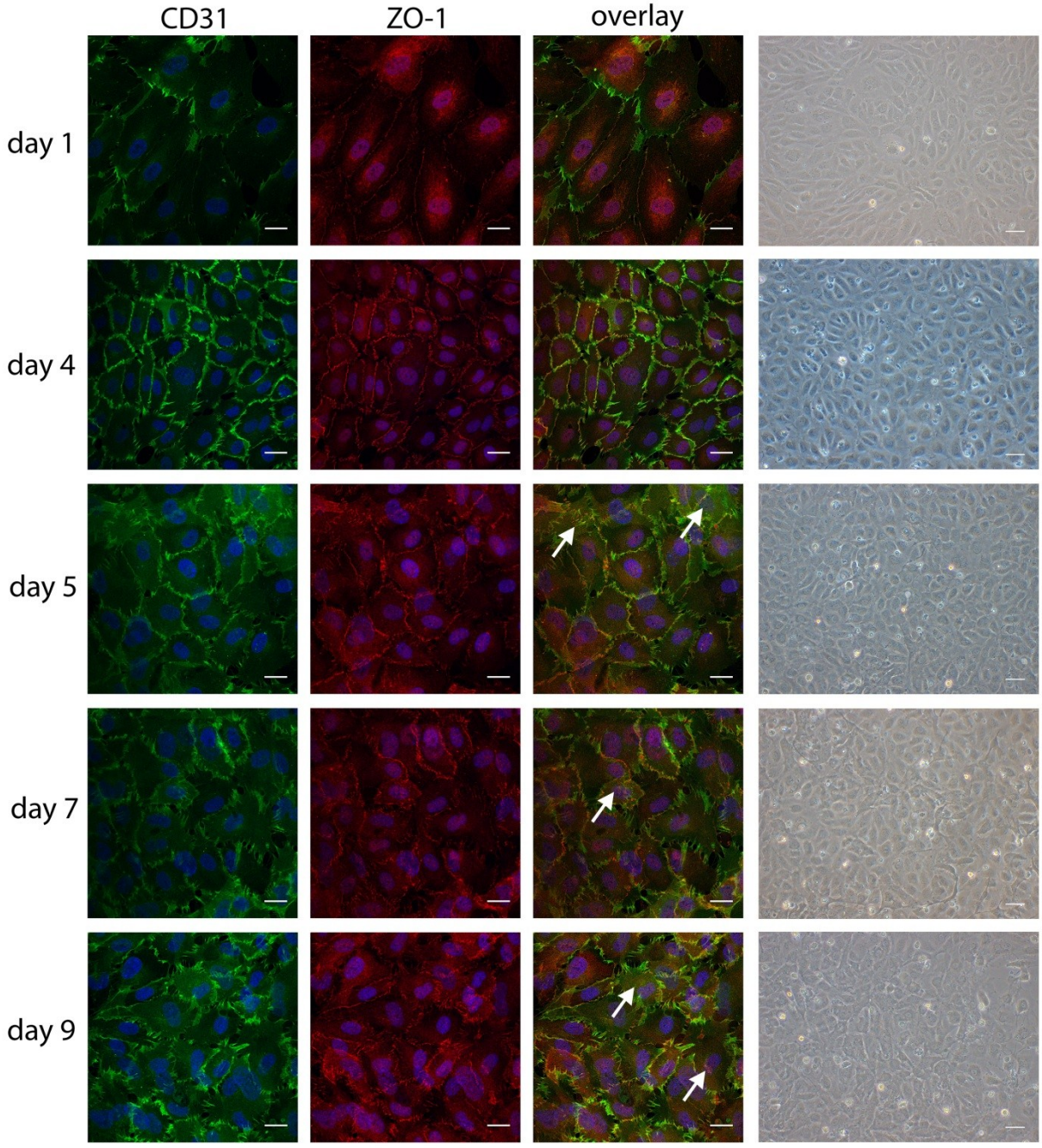


**Figure S3.** HUVEC barrier formation from high cell density cultures. 50000 cells $cm^{-2}$ HUVEC were plated on collagen coated glass coverslips and their growth was monitored for different days after seeding. Left: confocal images of HUVEC cells stained with anti-ZO-1 (red) or anti-CD31 (green) antibodies. Blue: DAPI stained nuclei (scale bar: 20 μm). Right: light microscopy images of the same cultures (scale bar: 50 μm). Tight junction staining showed barrier formation roughly 4 days after cell seeding, then cells started to overlap in multiple layers (as indicated by white arrows). Areas with holes in the cell monolayer were also observed, as a consequence of cell death.

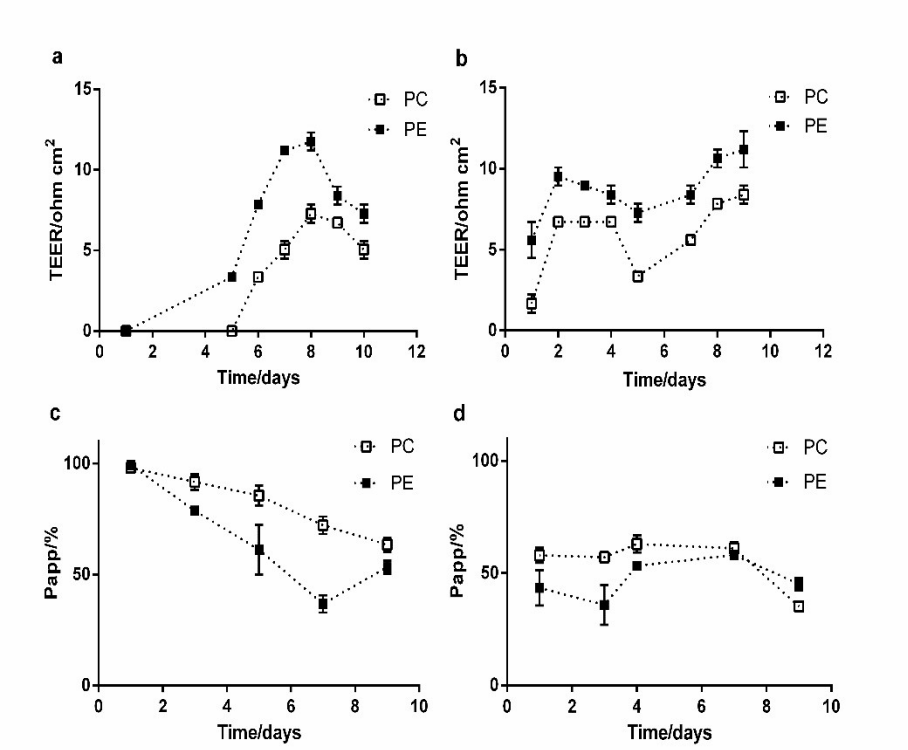


**Figure S4.** Optimization of HUVEC barrier formation. HUVEC were seeded at two concentrations (3000 cells cm$^{-2}$, (a) and (c) or 50000 cells cm$^{-2}$, (b) and (d)) on Transwell® inserts made of polyester (PE) or polycarbonate (PC) and barrier formation was monitored for several days after seeding**.** a, b: Trans Epithelial Electrical Resistance (TEER) at different times after seeding. Results are the average TEER value and standard deviation obtained from two different inserts which were measured over time for the entire experimental period. c, d: Apparent permeability ($P_{app}$) of FITC-Dextran (4 kDa, 200 µg ml$^{-1}$). The fluorescence intensity of FITC-Dextran in the basal chamber was used to calculate the apparent permeability as described in the Experimental Section. Results are the average value and standard deviation of 2 different inserts, normalized by the results obtained on Transwells without cells. Overall the results show that PE is a better substrate than PC for cell growth and barrier formation, and that seeding cells at lower density and waiting longer allowed HUVEC to develop into a cell barrier with high electrical resistance and a low permeability in about 7 days after seeding.

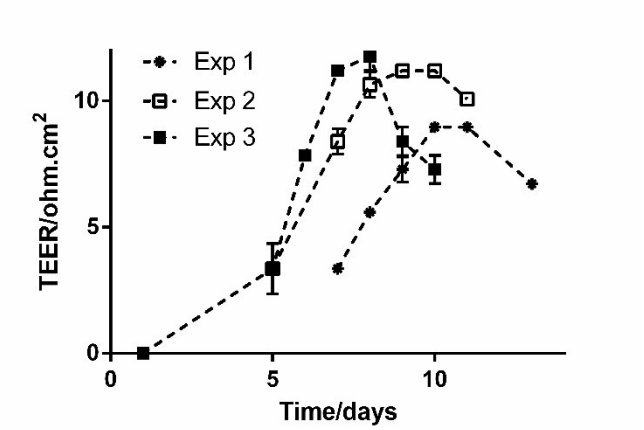


**Figure S5.** Trans Epithelial Electrical Resistance (TEER) of HUVEC layers formed on polyester (PE) filters. 3000 cells $cm^{-2}$. HUVEC were seeded on polyester Transwells as described in the Experimental Section and their TEER measured at the indicated times after seeding. Results are the average TEER value and standard deviation obtained from two different inserts which were measured over time for the entire experimental period. Even though in independent experiments the absolute TEER values were rather variable, the trend was consistent: in all cases, it showed a progressive increase of TEER at increasing days after seeding, with a peak reached 7-8 days after seeding, sign of barrier formation, followed by a progressive decrease as a consequence of cell death.

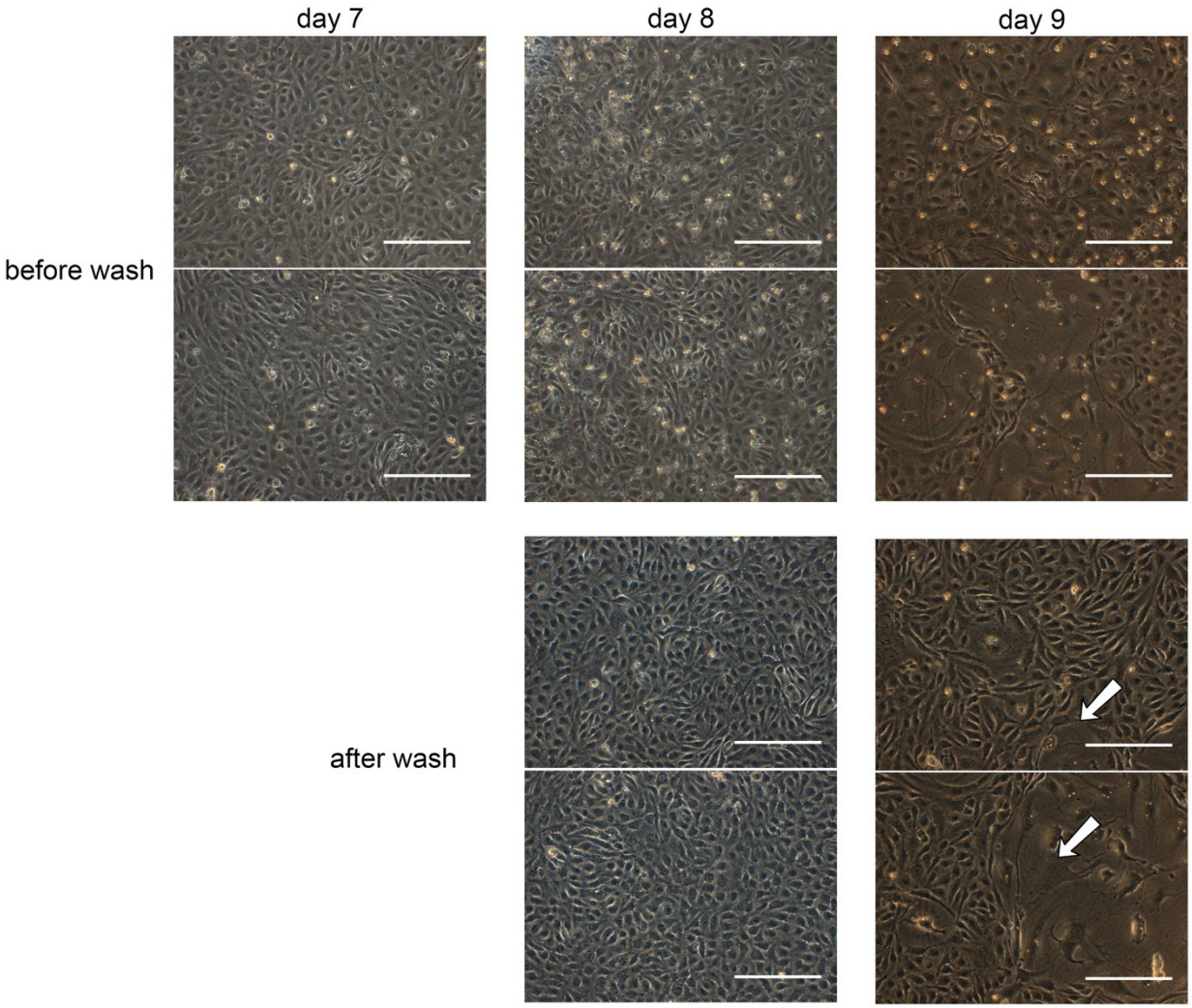


**Figure S6**. Integrity of HUVEC barriers formed from low cell density cultures. Representative light microscopy images before and after washing of HUVEC cell barriers formed from low cell density cultures, plated at a concentration of 3000 cells $cm^{-2}$ on 24 well plates and cultured for the indicated times (scale bar: 200 µm). Roughly 9 days after seeding, before washing the wells, many floating (dead) cells were clearly visible. Consecutively, after washing the wells, holes in the cell monolayer (as indicated by the white arrows) were visible. This overall indicated that in these conditions, roughly 9 days after cell seeding, barrier integrity was lost.

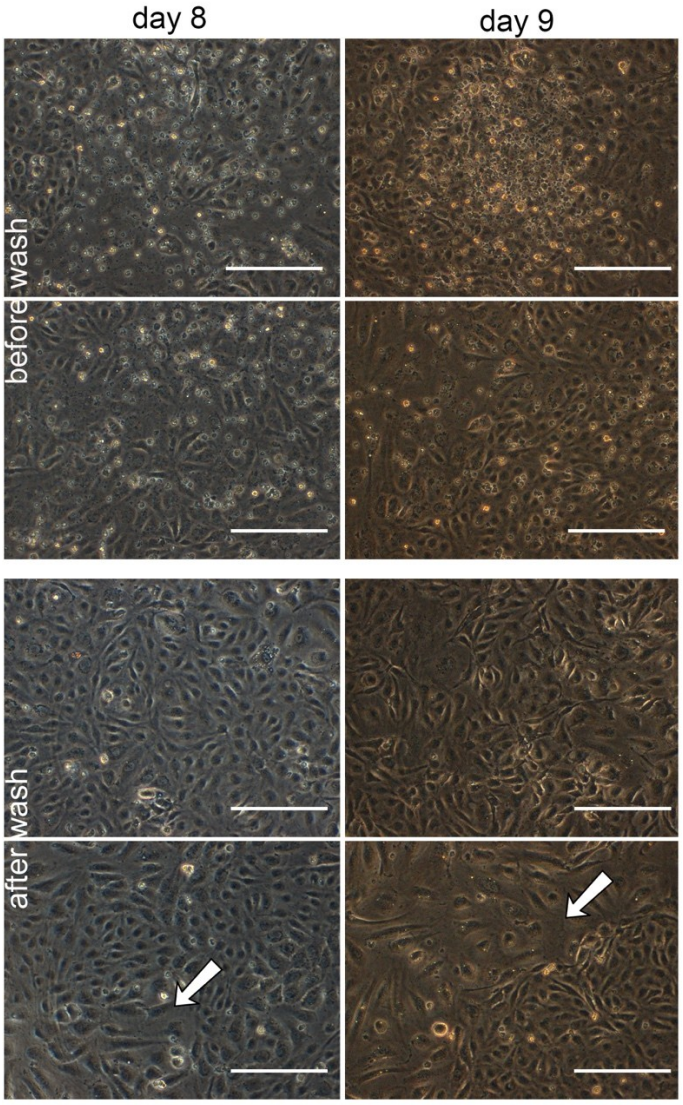


**Figure S7**. Integrity of HUVEC barriers formed from high cell density cultures. Representative light microscopy images before and after washing of HUVEC cell barriers formed from high cell density cultures, plated at a concentration of 50000 cells $cm^{-2}$ on 24 well plates and cultured for the indicated times (scale bar: 200 μm). Roughly 8 days after seeding, before washing the wells, many floating (dead) cells were clearly visible. Consecutively, after washing the wells, holes in the cell monolayer (as indicated by the white arrows) were visible. This overall indicated that in these conditions, roughly 8 days after cell seeding, barrier integrity was lost.

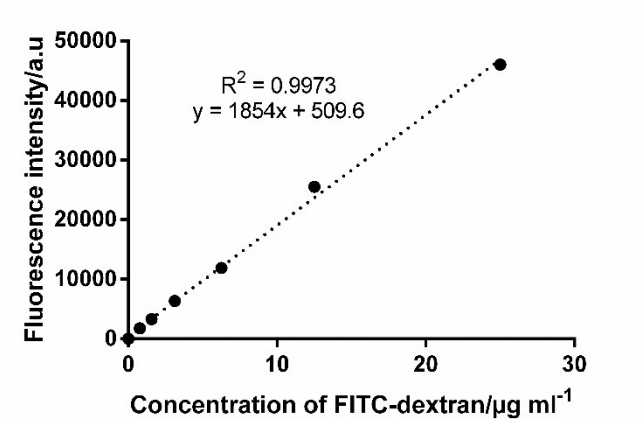


**Figure S8.** Calibration curve for FITC-Dextran fluorescence. The fluorescence intensity of samples at increasing concentrations of 4 kDa FITC-Dextran was measured using a spectrofluorometer. Linear regression was used to obtain the relation between FITC-dextran concentration and fluorescence, from which the apparent permeability $P_{app}$ was determined as described in the Experimental Section. A different calibration curve was made for each experiment ($R^2$ values $\geq 0.995$ in all cases).

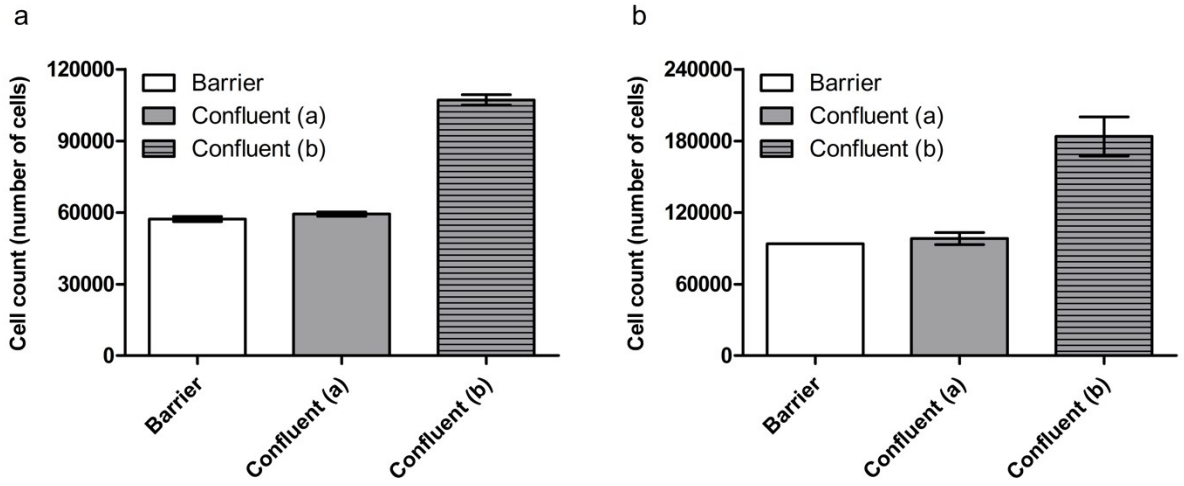


**Figure S9**. Number of cells in HUVEC barriers and confluent cell cultures. HUVEC barriers and confluent cultures were prepared by seeding 3000 cells $cm^{-2}$ (barrier) or 25000 cells $cm^{-2}$ (confluent (a)), and cell numbers were counted 7 days (barrier) or 1 day (confluent) after seeding. Additionally, 50000 cells $cm^{-2}$ (confluent (b)) were also seeded and cell numbers were counted 1 day after seeding, as ulterior control. Cell numbers were counted using a hemocytometer (a) or by flow cytometry (b) as described in the Experimental Section. The results are the average and standard deviation of two replicate wells. The results confirmed that the optimized cell barriers and confluent cell cultures (confluent (a)) had comparable cell numbers. When the double of cells was seeded (confluent (b)), a double number of cells was counted 1 day after seeding, further confirming accuracy in cell seeding and of the two methods used to count cell numbers.

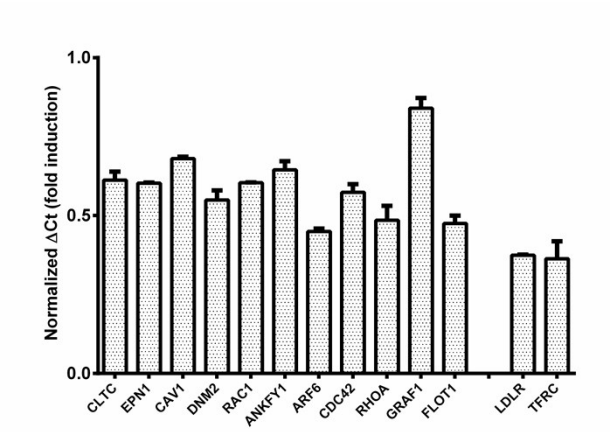


**Figure S10.** Expression levels of genes coding for endocytic proteins in HUVEC barriers in comparison to confluent cell cultures. HUVEC were seeded at a density of 3000 cells $cm^{-2}$ and cultured for 7 days (barriers). Alternatively, 25000 cells $cm^{-2}$ were seeded and cultured for 1 day (confluent cells). Then, RT-qPCR was performed as described in the Experimental Section to determine the expression levels of genes coding for cell receptors (LDL and transferrin receptors), and for a series of targets involved in clathrin mediated endocytosis (CME), caveolae-mediated endocytosis, macropinocytosis, and other clathrin and caveolae independent mechanisms (see also Supplementary Table S1 for details). Results are the average and standard deviation over 4 replicate wells of the fold-change in gene expression levels in HUVEC barriers compared to confluent cells. The results indicated that the gene expression of the selected endocytic targets in the cell barriers was lower than in confluent cells.

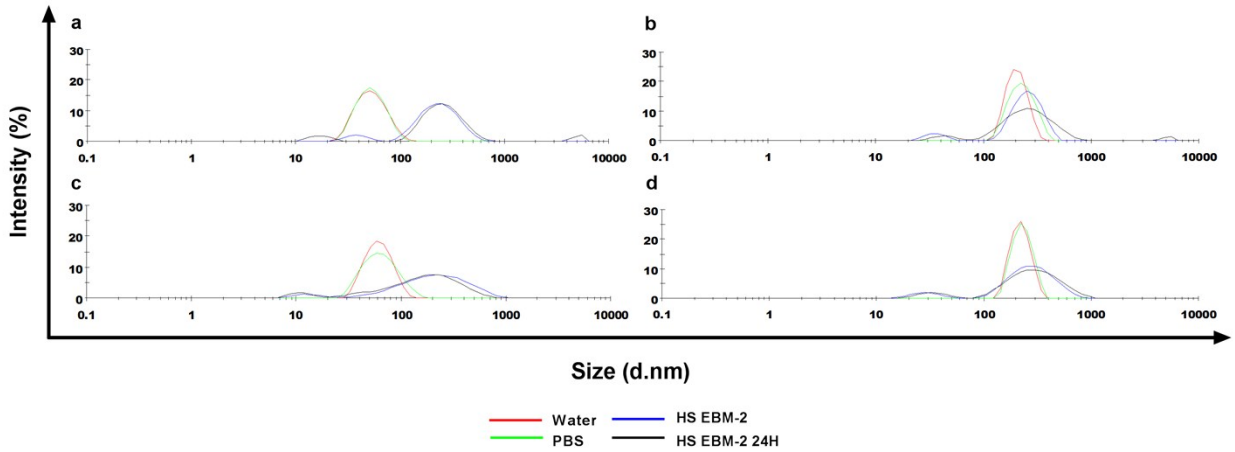


**Figure S11.** Size distribution by intensity (diameter, d, nm) of 50 nm red $SiO_2$ (**a**), 200 nm red $SiO_2$ (**b**), 40 nm red PS-COOH (**c**) and 200 nm orange PS-COOH (**d**) as obtained by dynamic light scattering (DLS). Silica nanoparticles (100 µg $ml^{-1}$) were dispersed in water, PBS, and EBM-2 supplemented with 4 mg $ml^{-1}$ of human serum (HS EBM-2). For the 40 nm PS-COOH nanoparticles instead (c), in order to determine the size distribution at a nanoparticle to protein ratio closer to that used for cell experiments, 25 µg $ml^{-1}$ nanoparticles were dispersed in EBM-2 supplemented with 50 mg $ml^{-1}$ human serum. For the same reasons, the 200 nm PS-COOH nanoparticles (d) were dispersed to a final concentration of 36 µg $ml^{-1}$ in EBM-2 supplemented with 48 mg $ml^{-1}$ human serum. Size distributions in HS EBM-2 were measured immediately, or after 24 hours of incubation of the dispersions at 37 ˚C, 5% $CO_2$ (HS EBM-2 24h). The results showed that all dispersions remained stable for up to 24 hours in the conditions used for cell experiments.

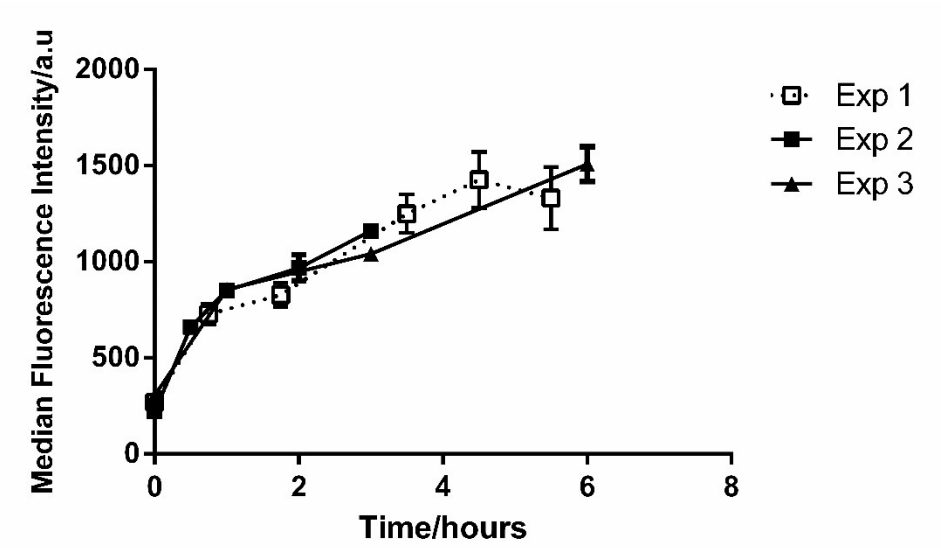


**Figure S12.** Reproducibility of nanoparticle uptake levels in HUVEC barriers in independent experiments. Median cell fluorescence intensity as obtained by flow cytometry of HUVEC barriers (7 days after seeding 3000 cells $cm^{-2}$) prepared in independent experiments (Exp 1-3) and exposed for increasing times to 100 μg $ml^{-1}$ 50 nm $SiO_2$ nanoparticles dispersed in EBM-2 medium supplemented with 4 mg $ml^{-1}$ human serum. (Exp 1 is from Figure 4f and Exp 2 is from Figure 4l, while Exp 3 is an equivalent independent replica). In the three independent experiments, barriers were formed following the optimized protocols and were exposed to independent nanoparticle dispersions, prepared as described in the Experimental Section, using nanoparticles and human serum from the same batches. Results are the average and standard deviation over three replicates of the median cell fluorescence intensities. Overall the results show that when the same nanoparticle stock and human serum were used to prepare the nanoparticle dispersions in independent experiments, a very good reproducibility in nanoparticle uptake in the cell barriers was obtained. This indicated a very good reproducibility of the barrier model, and also a very good control of the preparation of the nanoparticle dispersions, nanoparticle exposure to cells and sample preparation for measurement.

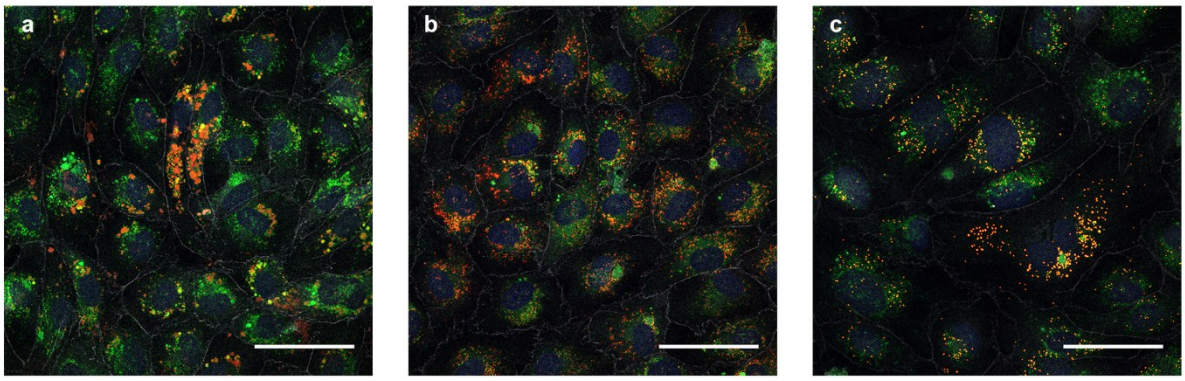


**Figure S13**. Uptake and intracellular distribution of different nanoparticles in HUVEC barriers. HUVEC barriers (7 days after seeding 3000 cells $cm^{-2}$) were exposed for 24 hours to 200 µg $ml^{-1}$ 200 nm $SiO_2$ (a), 2 µg $ml^{-1}$ 40 nm PS-COOH (b) or 3 µg $ml^{-1}$ 200 nm PS-COOH (c) nanoparticles in EBM-2 medium supplemented with 4 mg $ml^{-1}$ human serum. Red: nanoparticles, Green: LAMP-1, Grey: ZO-1, Blue: DAPI. Scale bar: 50 µm.

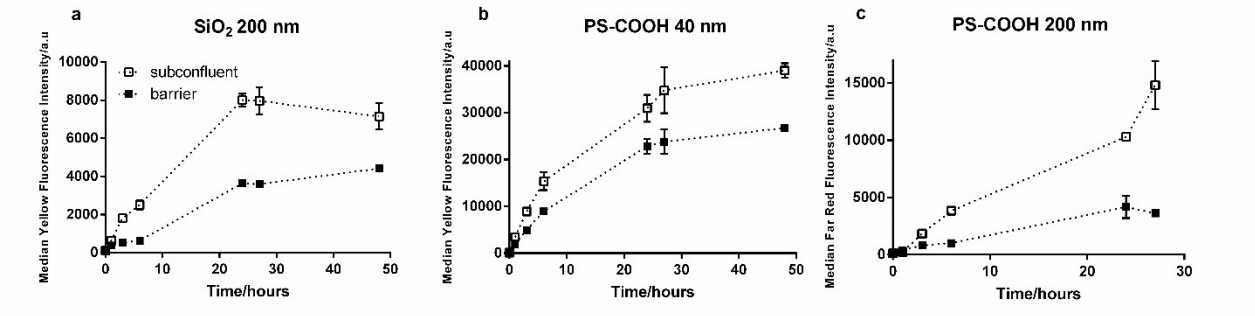


**Figure S14**. Nanoparticle uptake levels in HUVEC barriers and subconfluent cultures. Median cell fluorescence intensity as obtained by flow cytometry of HUVEC exposed to different nanoparticles. HUVEC were grown for 3 (subconfluent) or 7 (barrier) days after seeding (3000 cells $cm^{-2}$) and exposed to 200 nm $SiO_2$ (200 µg $ml^{-1}$, a), 40 nm PS-COOH (2 µg $ml^{-1}$, b) or 200 nm PS-COOH (3 µg $ml^{-1}$, c) in EBM-2 medium supplemented with 4 mg $ml^{-1}$ human serum for the indicated times. Results represent the average median and standard deviation of three replicates (for the 200 nm PS-COOH nanoparticles the far red fluorescence is shown because the yellow fluorescence in subconfluent cells was out of scale due to the extremely high fluorescence intensity of these nanoparticles and high uptake levels).

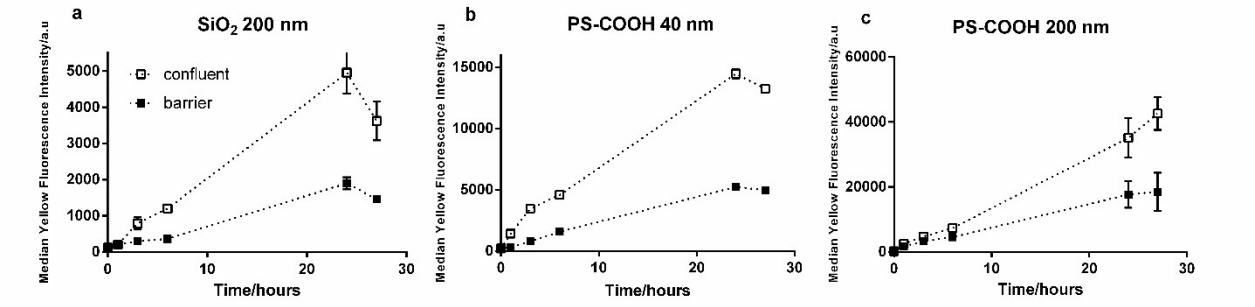


**Figure S15**. Nanoparticle uptake levels in HUVEC barriers and confluent cultures. Median cell fluorescence intensity as obtained by flow cytometry of HUVEC exposed to different nanoparticles. Confluent HUVEC (1 day after seeding 25000 cells $cm^{-2}$) and HUVEC barriers (7 days after seeding 3000 cells $cm^{-2}$) were exposed to 200 nm $SiO_2$ (200 µg $ml^{-1}$, a), 40 nm PS-COOH (2 µg $ml^{-1}$, b) or 200 nm PS-COOH (3 µg $ml^{-1}$, c) in EBM-2 medium supplemented with 4 mg $ml^{-1}$ human serum for the indicated times. Results represent the average median and standard deviation of three replicates.

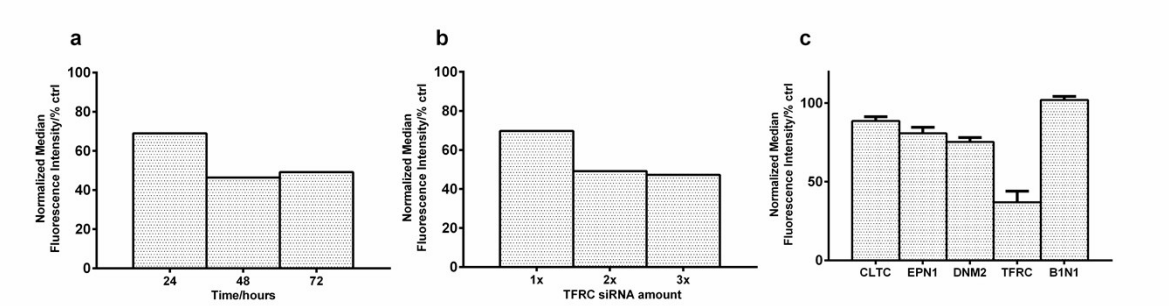


**Figure S16.** Silencing efficacy and uptake of transferrin in HUVEC transfected with siRNA to block the expression of the transferrin receptor (TFRC) and of other targets involved in clathrin mediated endocytosis (CME). 25000 cells $cm^{-2}$ HUVEC were seeded and grown for 24 hours. Silencing was performed following manufacturer's instructions, using a fixed amount of TFRC siRNA and of oligofectamine transfection reagent (1x corresponding to 10 pmol siRNA and 1 µl oligofectamine per well) for 24, 48 or 72 hours (a) or with increasing amounts of TFRC siRNA and transfection reagent (1x: 10 pmol siRNA and 1µl oligofectamine; 2x: 20 pmol siRNA and 2 µl oligofectamine; 3x: 30 pmol siRNA and 3 µl oligofectamine) for 72 hours (b). Silencing was also performed on other CME targets for 48 hours with a fixed amount of siRNA and transfection reagent (2x: 20 pmol siRNA and 2 µl oligofectamine) (c). After silencing, cells were exposed to 15 µg $ml^{-1}$ red fluorescent transferrin in serum free medium for 10 minutes and their fluorescence measured by flow cytometry. The results are the averaged median intensity and standard deviation over three replicates, normalized by the results in control cells silenced in the same way with a scramble siRNA (neg1 siRNA). In all cases transferrin uptake was reduced to a maximum of 50-60% in cells silenced for TFR in comparison to control cells, while up to 90% reduction can be obtained with the same method in cancer cells such as HeLa (data not shown). Transferrin uptake was barely affected in cells silenced for CME targets. Overall, this indicated low silencing efficacy in primary cells, in agreement with results in literature.

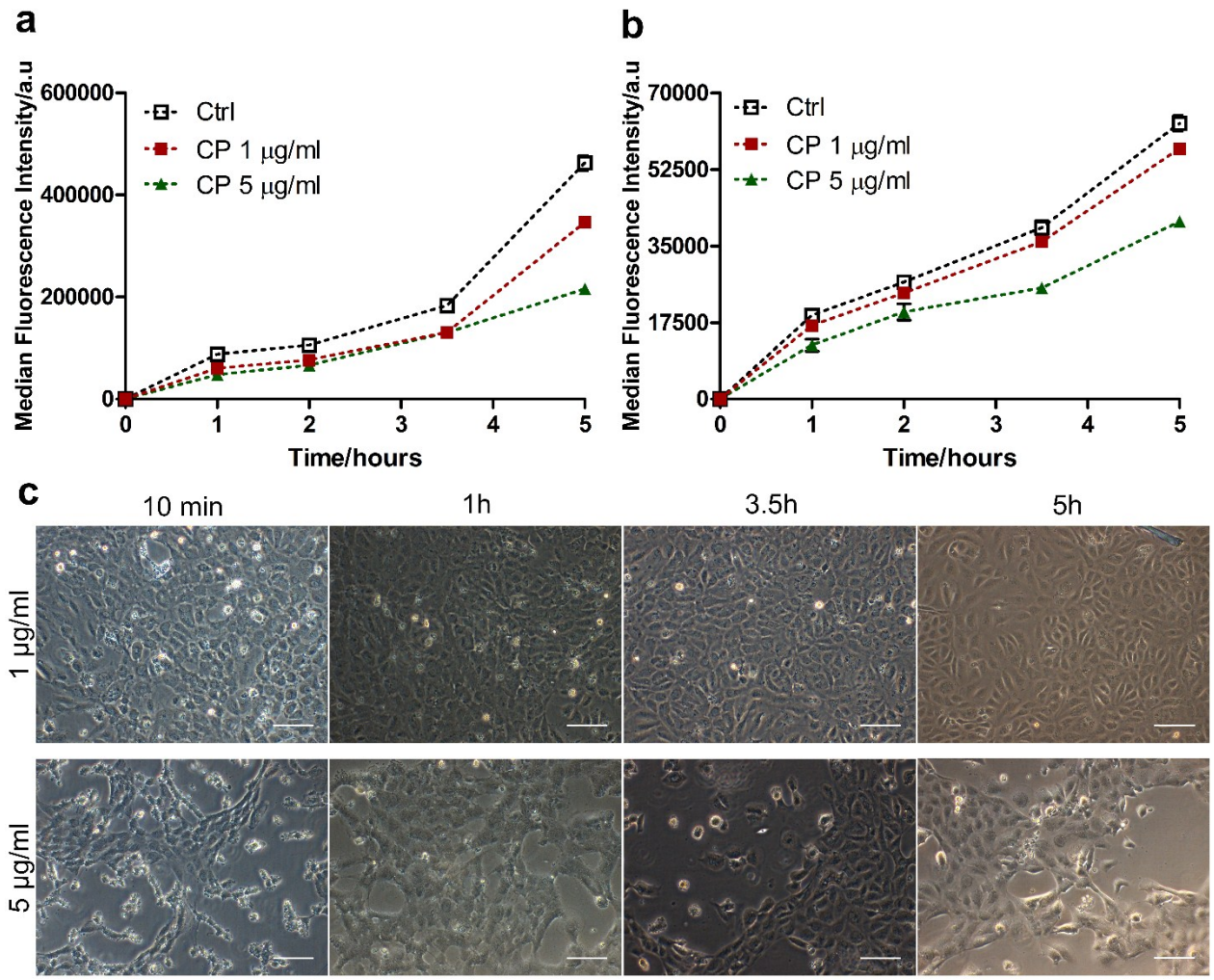


**Figure S17** Optimization of chlorpromazine (CP) dose on HUVEC barriers. HUVEC barriers (7 days after seeding 3000 cells $cm^{-2}$) were exposed to 1 or 5 µg $ml^{-1}$ CP. Efficacy of CP (a) and effect of CP on nanoparticle uptake (b) were assessed by measuring the uptake of 2 µg $ml^{-1}$ BODIPY LDL and 100 µg $ml^{-1}$ 50 nm red $SiO_2$ nanoparticles in EBM-2 supplemented with 4 mg $ml^{-1}$ human serum, respectively, for the indicated doses and times in the presence or absence of CP. Results are the average and standard deviation of three replicates. Light microscopy images of HUVEC barriers (c) were taken to monitor the effect of CP on HUVEC barrier integrity after exposure for the indicated times to the different CP doses (scale bar: 100 µm). The results showed that in all conditions tested, exposure to CP resulted in loss of barrier integrity. Furthermore, at the lower dose tested, CP efficacy in blocking LDL uptake was minimal. Thus, 5 µg $ml^{-1}$ CP was selected for further experiments on cell barriers, to ensure at least a partial inhibition, even if this dose led inevitably to loss of barrier integrity.

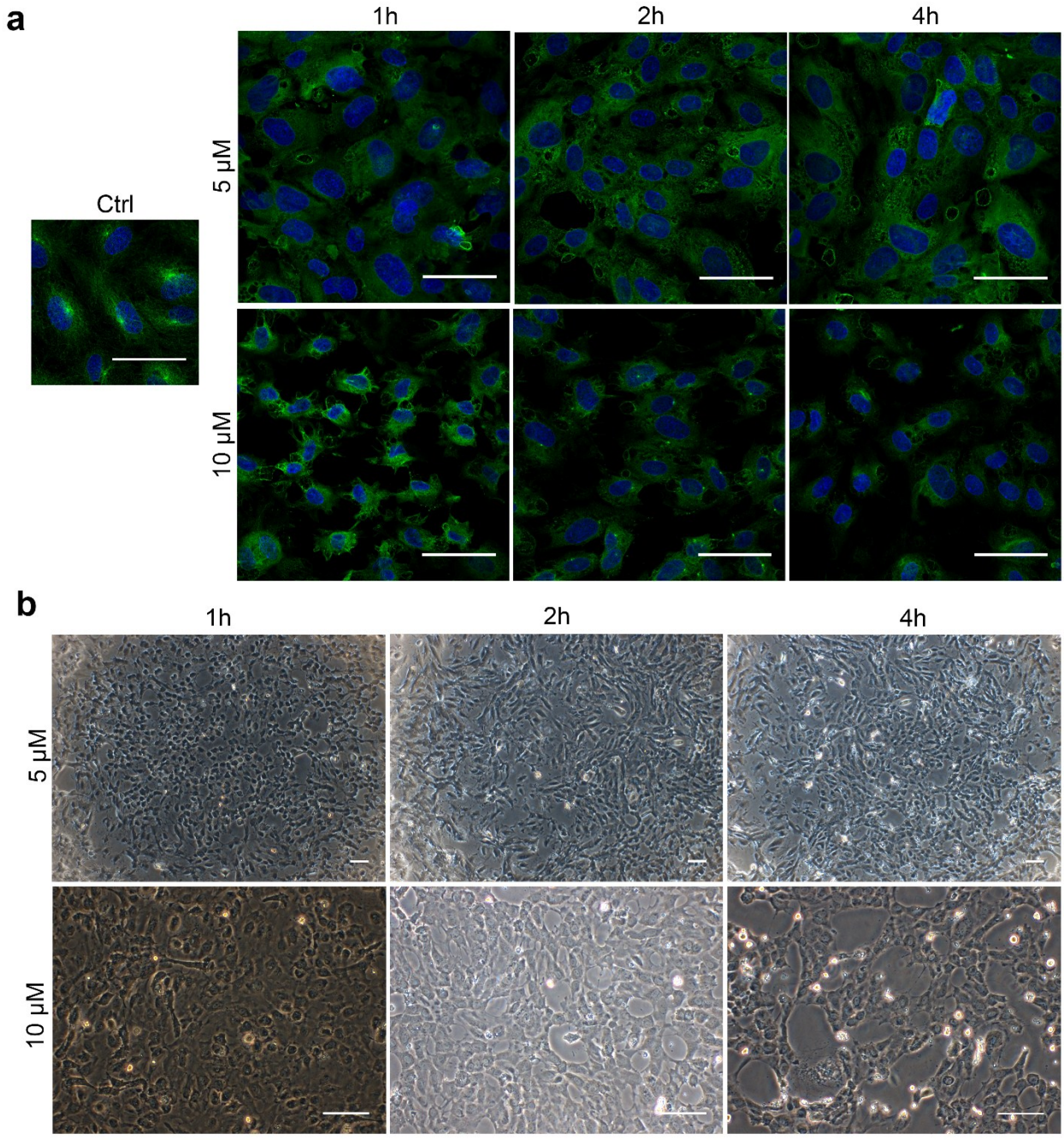


**Figure S18**. Optimization of nocodazole (NZ) dose on HUVEC barriers. HUVEC barriers (7 days after seeding 3000 cells $cm^{-2}$) were exposed to 5 or 10 µM NZ. (a) Confocal images after staining the cells with fluorescent antibodies against tubulin were taken on untreated control barriers (Ctrl) and barriers exposed to the different doses of NZ for the indicate times (scale bar: 50 µm). Light microscopy images of HUVEC barriers (b) were taken after exposure for the indicated times to the different NZ doses to monitor the effect on HUVEC barrier integrity (scale bar: 100 µm). The results showed that even at the lower dose tested, exposure to NZ led to loss of barrier integrity. It is likely that loss of microtubules as induced by this compound leads inevitably to loss of barrier integrity (the tested doses are already much lower than what usually applied for this kind of compounds).[36]

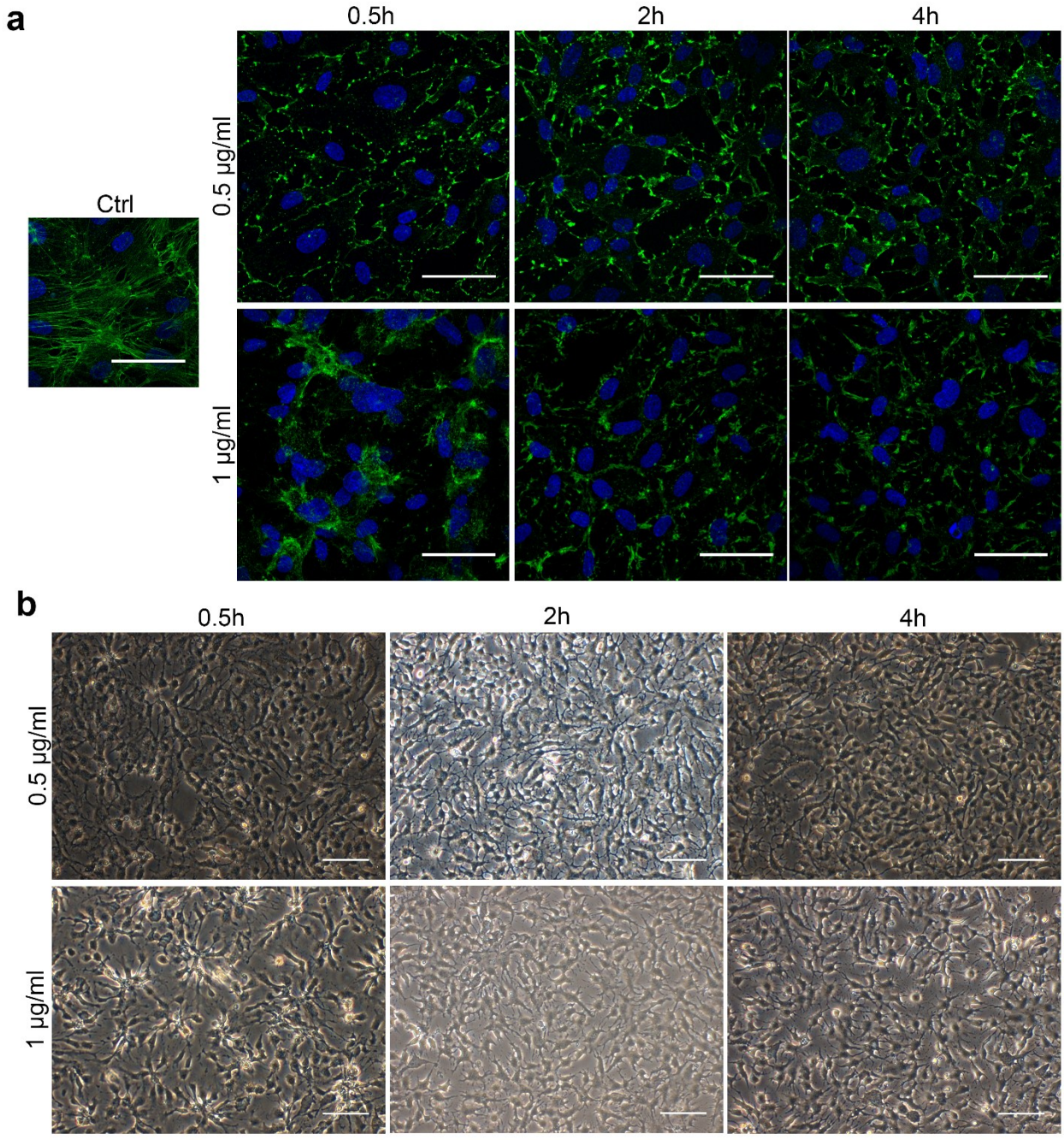


**Figure S19**. Optimization of cytochalasin D (CytoD) dose on HUVEC barriers. HUVEC barriers (7 days after seeding 3000 cells $cm^{-2}$) were exposed to 0.5 or 1 µg $ml^{-1}$ CytoD. (a) Confocal images after actin staining (performed as described in the Experimental Section) were taken on untreated control barriers (Ctrl) and barriers exposed to the different doses of CytoD for the indicated times (scale bar: 50 µm). Light microscopy images of HUVEC barriers (b) were taken after exposure for the indicated times to the different CytoD doses to show the effect on HUVEC barrier integrity (scale bar: 100 µm). The results showed that even at the lower dose tested, exposure to CytoD led to loss of barrier integrity. It is likely that loss of actin as induced by this compound leads inevitably to loss of barrier integrity (the tested doses are already much lower than what usually applied for this kind of compounds).[36]

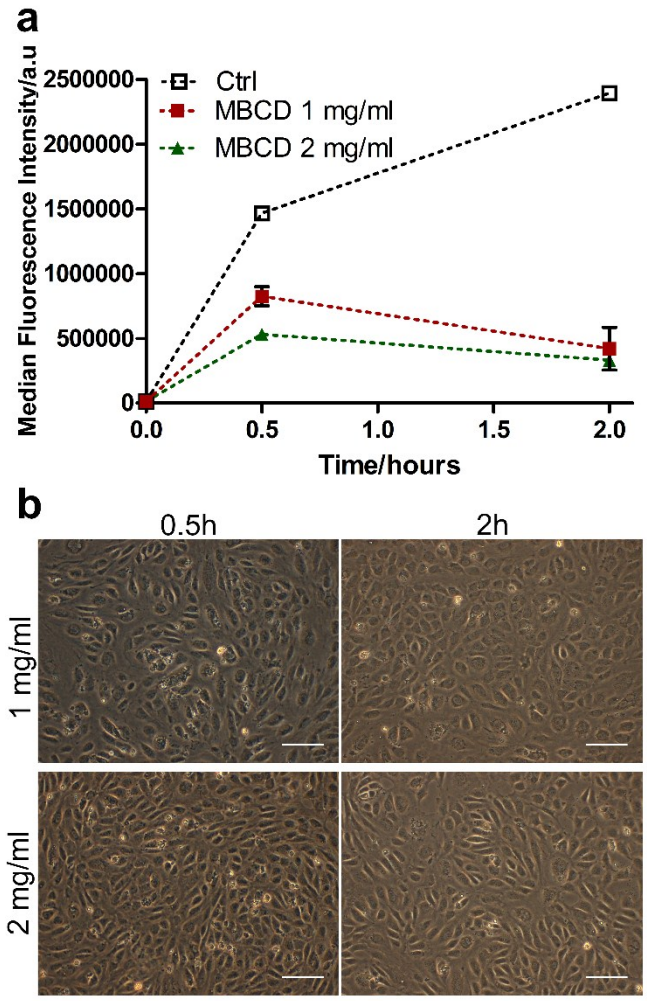


**Figure S20**. Optimization of methyl-β-cyclodextrin (MBCD) dose on HUVEC barriers. HUVEC barriers (7 days after seeding 3000 cells $cm^{-2}$) were exposed to 1 or 2 mg $ml^{-1}$ MBCD. Efficacy of MBCD (a) was assessed by measuring the uptake of 1 µg $ml^{-1}$ BODIPY LacCer for the indicated doses and times in the presence or absence of MBCD. Results are the average and standard deviation of three replicates. Light microscopy images of HUVEC barriers (b) were taken after exposure for the indicated times to the different MBCD doses to monitor the effect on HUVEC barrier integrity (scale bar: 100 µm). The results showed that in all conditions tested MBCD efficacy in blocking LacCer uptake was optimal, and barrier integrity was maintained.

.

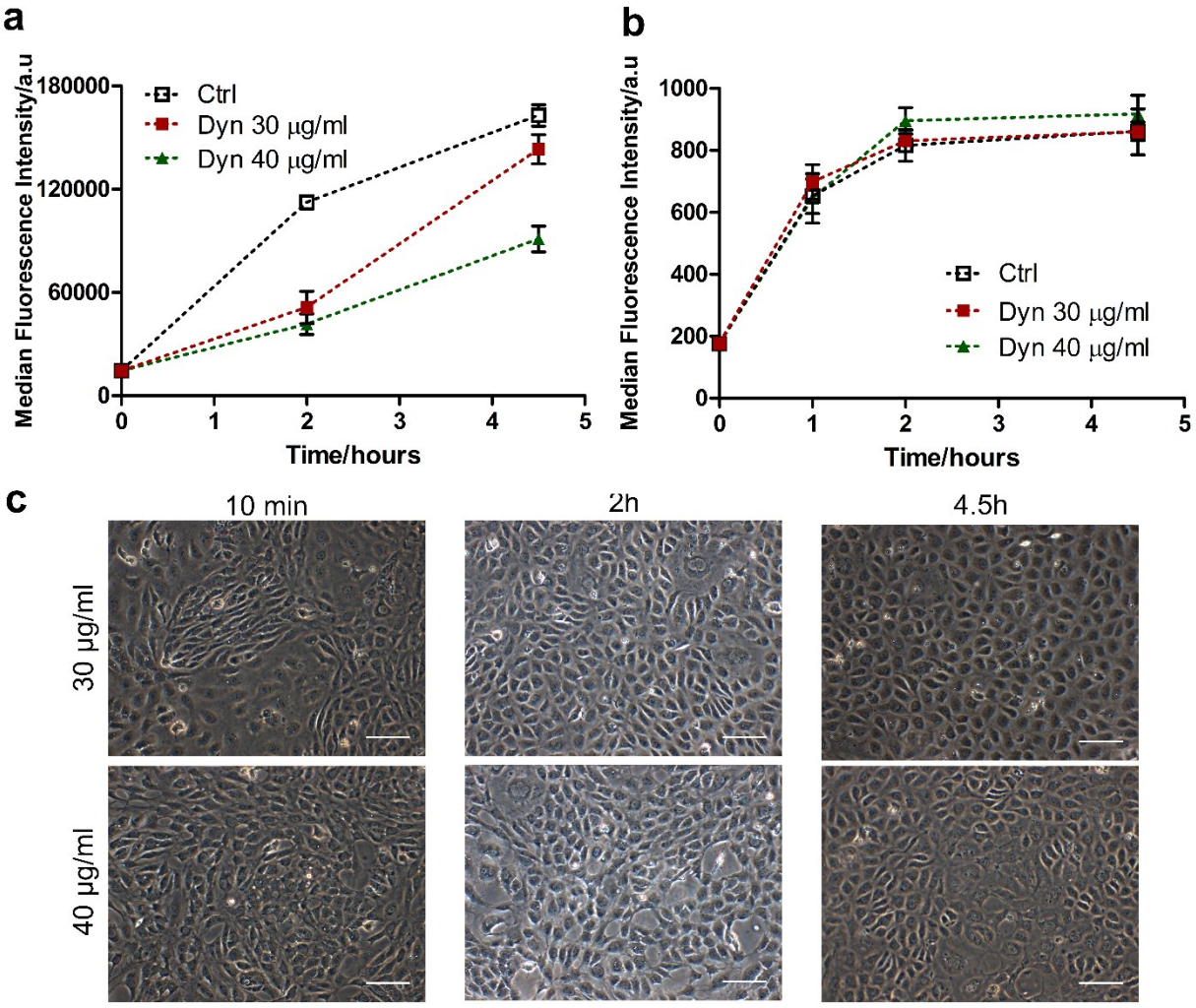


**Figure S21**. Optimization of dynasore (Dyn) dose on HUVEC barriers. HUVEC barriers (7 days after seeding 3000 cells $cm^{-2}$) were exposed to 30 or 40 µg $ml^{-1}$ Dyn. Efficacy of Dyn (a) and effect of Dyn on nanoparticle uptake (b) were assessed by measuring the uptake of 2 µg $ml^{-1}$ BODIPY LDL and 100 µg $ml^{-1}$ 50 nm red $SiO_2$ nanoparticles in EBM-2 supplemented with 4 mg $ml^{-1}$ human serum, respectively, in the presence or absence of Dyn. Results are the average and standard deviation of three replicates. Light microscopy images of HUVEC barriers (c) were taken after exposure for the indicated times to the different Dyn doses to monitor the effect on HUVEC barrier integrity (scale bar: 100 µm). The results showed that in all conditions tested Dyn efficacy in blocking LDL uptake was high, and barrier integrity was maintained.

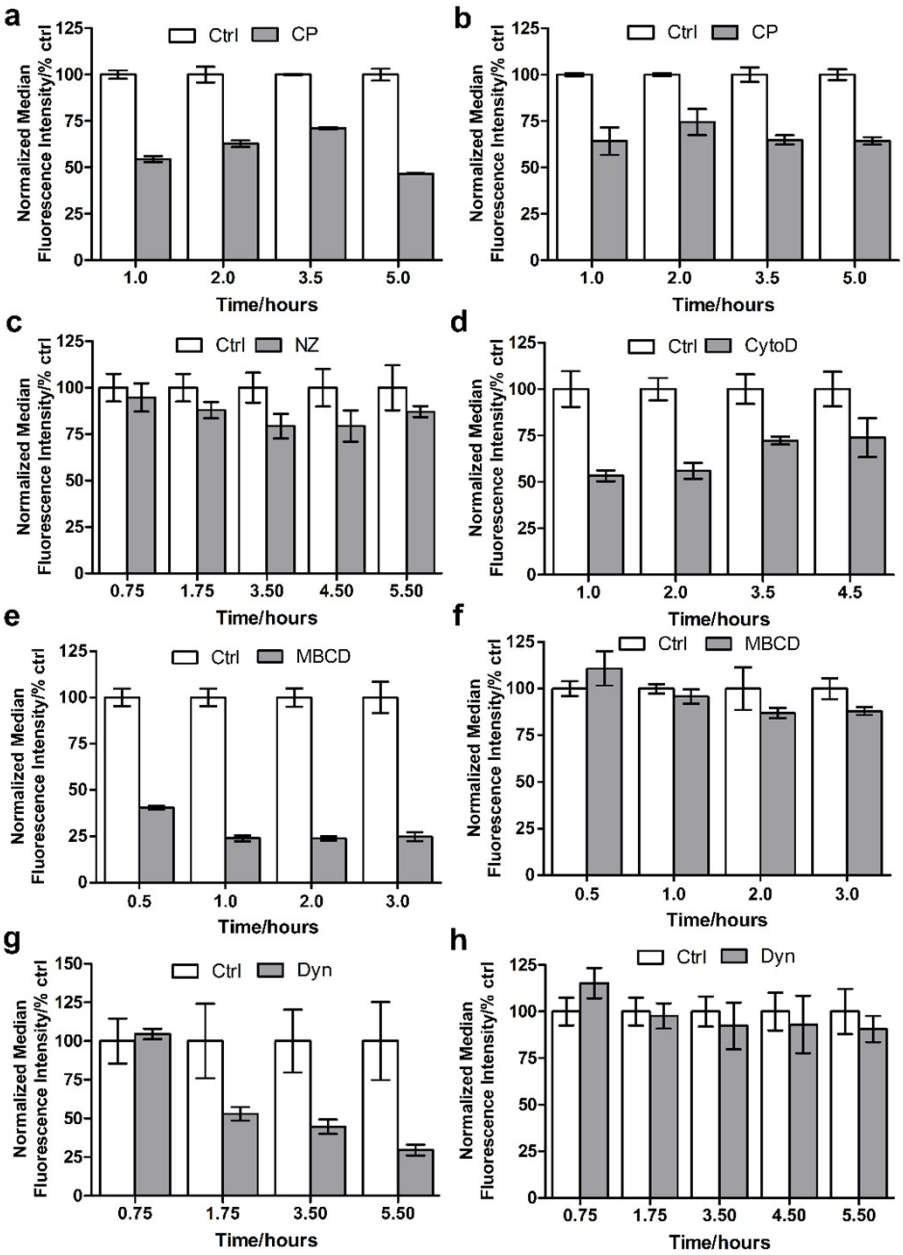


**Figure S22.** Normalized uptake levels in HUVEC barriers exposed to different inhibitors. The same data of Figure 4 are shown here after normalization for the uptake in control cells without inhibitors. HUVEC barriers (7 days after seeding 3000 cells $cm^{-2}$) were exposed to 5 μg $ml^{-1}$ chlorpromazine (CP) (a and b), 5 μM nocodazole (NZ) (c), 0.5 μg $ml^{-1}$ cytochalasin D (CytoD) (d), 2 mg $ml^{-1}$ methyl-β-cyclodextrin (MBCD) (e and f), or 30 μg $ml^{-1}$ dynasore (Dyn) (g and h). Left panels (a, e and g): uptake by flow cytometry of 2 μg $ml^{-1}$ BODIPY LDL (a and g), and 1 μg $ml^{-1}$ of BODIPY LacCer (e) in control cells (Ctrl) and cells exposed to chlorpromazine, dynasore and MβCD respectively, as a control for drug efficacy. Right panels (b, d, f and h) and c: effect of the drugs on nanoparticle uptake. HUVEC barriers were exposed to 100 μg $ml^{-1}$ 50 nm red $SiO_2$ nanoparticles in EBM-2 supplemented with 4 mg $ml^{-1}$ human serum for the indicated times in the presence or absence of the different drugs. The results are the average and standard deviation of three replicates, normalized by the uptake in control cells without inhibitors.

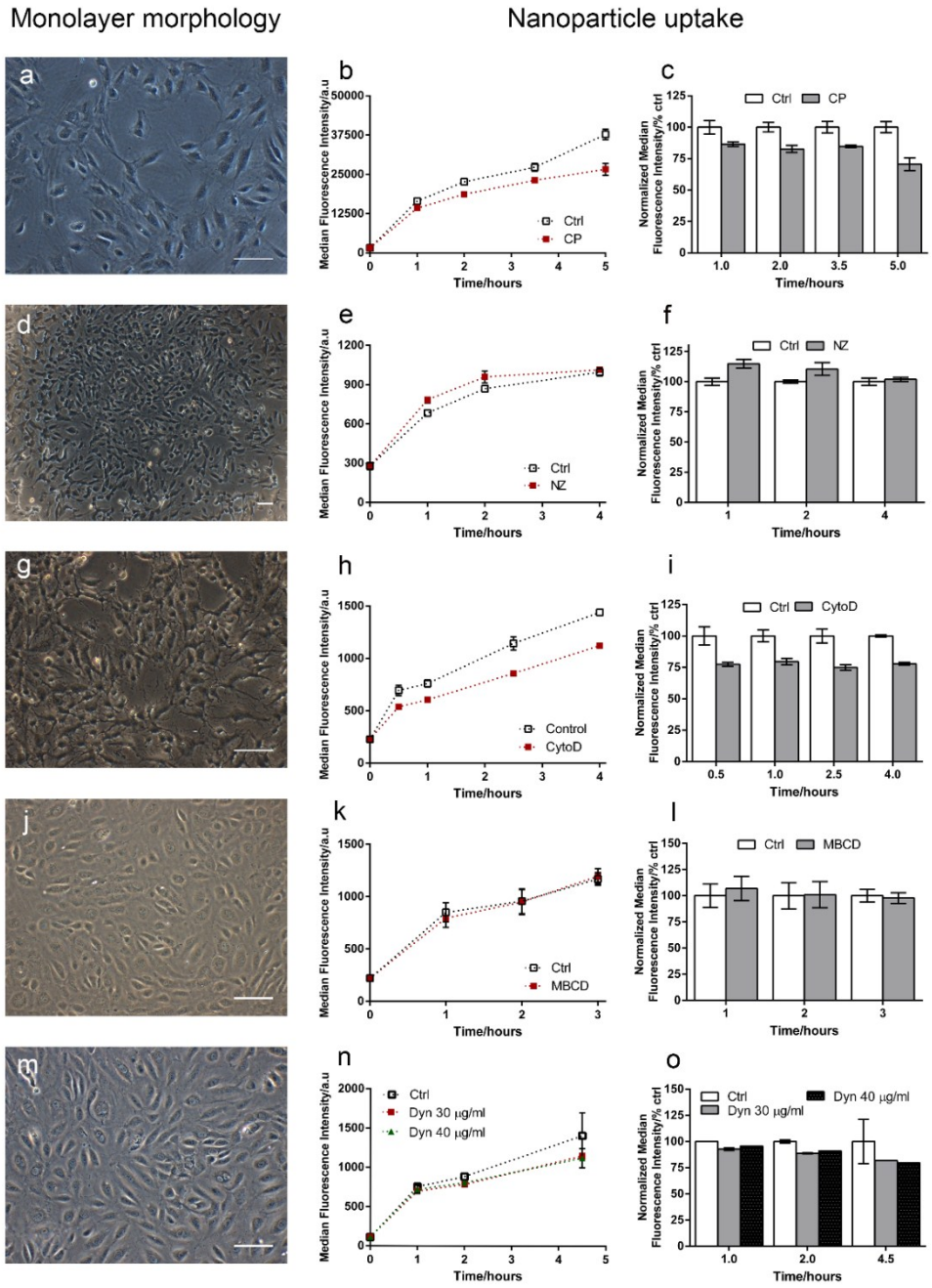


**Figure S23**. Uptake mechanisms in confluent HUVEC cells. Confluent HUVEC cells (1 day after seeding 25000 cells $cm^{-2}$) were exposed to 5 µg $ml^{-1}$ chlorpromazine (CP) (a-c), 5 µM nocodazole (NZ) (d-f), 0.5 µg $ml^{-1}$ cytochalasin D (CytoD) (g-i), 2 mg $ml^{-1}$ methyl-β-cyclodextrin (MBCD) (j-l), or 30 µg $ml^{-1}$ dynasore (Dyn) (m-o). Left panels: light microscopy images of confluent HUVEC cell morphology after exposure to each inhibitor (scale bar: 100 µm). Middle panels: effect of the inhibitors on nanoparticle uptake. Confluent HUVEC cells were exposed to 100 µg $ml^{-1}$ 50 nm $SiO_2$ nanoparticles in EBM-2 supplemented with 4 mg $ml^{-1}$ human serum for the indicated times in the presence or absence (Ctrl) of the different inhibitors. Results are the average and standard deviation of three replicates. Right panels: the same nanoparticle uptake results, normalized for uptake levels in control cells without inhibitors.